Available online at www.sciencedirect.com
SCIENCE DIRECT
European Journal of Pharmaceutics and Biopharmaceutics 62 (2006) 306–314
European Journal of Pharmaceutics and Biopharmaceutics
www.elsevier.com/locate/ejpb

Research paper

In vitro uptake of gelatin nanoparticles by murine dendritic cells and their intracellular localisation

Conrad Coester [a,b,*], Paras Nayyar [a], John Samuel [a]

[a] Faculty of Pharmacy and Pharmaceutical Sciences, 3118 Dentistry/Pharmacy Centre, University of Alberta, Edmonton, Alberta, Canada
[b] Department of Pharmacy, Ludwig-Maximilians University, Munich, Germany

Received 30 March 2005; accepted in revised form 27 September 2005
Available online 28 November 2005

Abstract

The long term goal of this study is to develop an efficient nanoscopic vaccine delivery system, based on the biodegradable and natural polymer gelatin, to deliver therapeutic protein antigens along with adjuvants into dendritic cells (DCs). In this study, gelatin nanoparticles were tested for qualitative and quantitative uptake in murine DCs in vitro. A second aim of this study was to prove that the carrier system is able to deliver tetramethylrhodamine conjugated dextran (TMR–dextran), as a model drug into the DCs. The TMR–dextran was incorporated during the preparation of the gelatin nanoparticles. DCs were generated from murine bone marrow cells by an established ex vivo technique. Flow cytometry showed that 88% of the cells positive for the specific murine DC marker CD11c took up TMR–dextran loaded gelatin nanoparticles, whereas only 4% of the soluble form of TMR–dextran was taken up. Double color confocal laser scanning microscopy (CLSM) showed that gelatin nanoparticles were phagocytosed by DCs and the triple color CLSM showed that the TMR–dextran was localized mainly in lysosomes as expected, but partly also outside the lysosomes, presumably in the cytoplasm. An in vitro release study of TMR–dextran from gelatin nanoparticles demonstrated that there was hardly any release in phosphate buffered saline (PBS), but by trypsin-assisted degradation of gelatin nanoparticles resulted in the release of about 80% of the TMR–dextran from the particles. These results suggest that gelatin nanoparticles hold promise as a new biocompatible tool for vaccine delivery to DCs, with applications in cancer immunotherapy.

Keywords: Dendritic cells; Gelatin; Nanoparticles; Tetramethylrhodamine dextran; Phagocytosis; Intracellular localisation; Cancer vaccination

1. Introduction

Dendritic cells (DCs) are called as the 'professional antigen presenting cells (APCs)' as they are most proficient in capturing, processing and presentation of antigens, and triggering T-cell mediated immune responses. They are also the only APCs capable of primary activation of naïve T lymphocytes [1]. Administration of antigens or drugs in soluble forms results in their broad distribution in the body and is inefficient in targeting APCs. Antigen delivery in colloidal carrier systems leads to higher uptake by APCs as compared to its soluble form [2,3] and consequently causes higher immune responses [4,5]. This may be due to the difference in the uptake mechanism of particulate (via phagocytosis) and soluble forms of antigens (pinocytosis) by DCs [6]. Hence, there is a need for efficient particulate delivery systems that can selectively target APCs, in particular DCs, for generating effective immune responses. Vaccination with antigen-loaded DCs holds immense potential for the treatment of cancer [7–9]. Two approaches can be followed to use DCs for cancer immunotherapy. The first approach is to directly inject the particulate formulation loaded with cancer antigens to facilitate capturing of antigens by immature DCs. Immature DCs have a high level of phagocytic activity. The uptake of antigens leads to the maturation and upregulation of a number of molecules including CD11c, CD 40, CD80, CD83, CD86, MHC II and IL-12 [10]. These DCs then migrate to the draining lymph nodes via afferent lymphatics and finally to T cell areas, where they present processed antigens, in association with MHC class I and class II molecules, to the naïve T cells leading to antigen specific T cell responses [11]. T cell mediated immune responses, specifically Th1 and cytotoxic T lymphocyte (CTL) responses are required to fight viral infections and cancer [12]. The second approach involves ex vivo delivery of tumor-associated antigens to DCs, usually generated from

* Corresponding author. Department of Pharmacy, Ludwig-Maximilians University, Pharmaceutical Technology and Biopharmacy, Butenandtstr. 5-13 Building B, 81377 Munich, Germany. Tel: +49 89 2180 77025; fax: +49 89 2180 77026.
E-mail address: conrad.coester@cup.uni-munechen.de (C. Coester).

0939-6411/$ - see front matter © 2006 Elsevier B.V. All rights reserved.
doi:10.1016/j.ejpb.2005.09.009

peripheral blood monocytes ex vivo and the re-administration of antigen-loaded DCs to cancer patients for the activation of tumor-specific immune responses. Preclinical studies have demonstrated that DCs, loaded with tumor antigens ex vivo can elicit T cell-mediated tumor destruction in vitro and in vivo [13,14]. Therefore, safe vaccine delivery system that can efficiently deliver antigens to DCs are of major significance to cancer immunotherapeutic strategies. In the present study, murine DCs were used as an in vitro model as they are easily and reproducibly generated in large quantities from murine bone marrow, amenable to detailed characterization based on surface markers, and widely accepted as a preclinical model in immunotherapy studies.

Nanoparticles possess certain advantages over the liposomal delivery systems, such as greater stability during storage, stability in vivo after administration and ease of scale-up during manufacture [15]. On the other hand, some liposomal medications have already been approved and are commercially available. This might be due to lack of biocompatibility of the synthetic polymers used for the preparation of nanoparticles. Gelatin has a better chance to be approved as a biopolymer for nanoparticles since it has been used for decades as plasma expander. Peptide antigens can be encapsulated in biodegradable nanoparticles for targeted delivery and sustained release of antigens to DCs and enhanced immune responses. Lutsiak et al. were able to demonstrate that poly(lactic-*co*-glycolic acid) (PLGA) nanospheres are efficient vaccine delivery systems for targeting human DCs [16]. Biodegradable nanoparticulate carriers based on gelatin may offer another system for targeted delivery of antigens to DCs. Gelatin is a natural macromolecule originating from collagen contained in animal bones and skin. It is biodegradable, non-toxic, easy to crosslink and to modify chemically and has therefore an immense potential to be used for the preparation of colloidal drug delivery systems such as microspheres and nanoparticles. Other advantages are: it is inexpensive, can be sterilized, is not usually contaminated with pyrogens and possesses relatively low antigenicity [17]. It has been used for decades in parenteral formulations and is an approved plasma expander [18,19]. The purpose of this study was to quantify the uptake of gelatin nanoparticles by murine DCs using flow cytometry and to demonstrate the intracellular distribution of the model drug tetramethylrhodamine-conjugated dextran (TMR–dextran) using triple color confocal laser scanning microscopy (CLSM). Additionally, the release of TMR–dextran from the nanoparticulate formulation was analyzed in phosphate buffered saline (PBS), with and without enzyme (trypsin–EDTA) at 37 °C, in order to study the release kinetics of the model drug in different environments. For conducting these studies, TMR–dextran was incorporated in gelatin nanoparticles using a new method.

2. Materials and methods

2.1. Preparation of gelatin nanoparticles

The unloaded gelatin nanoparticles were prepared by the two-step desolvation method [20]. 1.25 g of gelatin type A (porcine skin, 175 bloom, Sigma Chemical Co., St Louis, USA) was dissolved in 25 ml of highly purified water (milliQ™ water) and the solution was heated until a clear gelatin solution was achieved. The gelatin was then desolvated by adding 25 ml of acetone (always p.a. quality) and sedimented for a short time. The supernatant containing dissolved and dispersed gelatin was then discarded. The sediment was re-dissolved in 25 ml of milliQ™ water at 55 °C and the pH of the solution was made acidic (pH 2.5) by adding 200 μl of 1 M hydrochloric acid. The gelatin was then again desolvated by dropwise addition of 55 ml of acetone. After 5 min of stirring, 400 μl of glutaraldehyde (25%) was added to the above system to crosslink the in-situ nanoparticles. The dispersion was stirred overnight until most of the acetone was evaporated and then purified by threefold centrifugation and redispersion in 30% acetone in milliQ™ water. After the third centrifugation, the particles were redispersed in pure milliQ™ water.

2.2. Preparation of TMR–dextran loaded gelatin nanoparticles

0.625 g of gelatin type A was dissolved in 12.5 ml of milliQ™ water at 55 °C until a clear gelatin solution was formed. The gelatin was then desolvated by adding 12.5 ml of acetone and sedimented for a short time. The supernatant was discarded and the sediment re-dissolved in12.5 ml water at 55 °C and 100 μl of 1 M sodium hydroxide solution added. 2.5 mg of TMR–dextran (mol. wt-40,000 daltons; Molecular probes, Eugene, USA) in 100 μl phosphate-buffered saline (PBS) was added to the system and the gelatin was co-acervated with TMR–dextran by dropwise addition of acetone (30 ml) until a dark pink colored precipitate was formed. The colorless supernatant was removed and the colored precipitate was re-dissolved in 12.5 ml of water under heating. The pH of the colored solution was made acidic (pH 2.5) by adding 120 μl of hydrochloric acid. The final TMR–dextran loaded nanoparticles were formed by dropwise addition of 35 ml acetone. After 5 min of stirring, 200 μl of glutaraldehyde (25%) was added to crosslink the in-situ nanoparticles. After 2 h of stirring, the nanoparticles were purified by centrifugation and redispersion in 30% acetone in milliQ™ water until the supernatant was colorless. Finally, the nanoparticles were redispersed in milliQ™ water.

2.3. Characterization of nanoparticles

The concentration of the nanoparticles was determined gravimetrically by drying 500 μl dispersion in an oven at 60 °C overnight until the weight was constant. Particle size for unloaded and TMR-loaded particles was determined by photon correlation spectroscopy (PCS) using a Zetasizer 3000 HSA (Malvern, UK); 100 μl of the NP dispersion (∼20 mg/ml) was mixed with 3.0 ml of milliQ™ water in the measuring cuvette.

2.3.1. Determination of TMR–dextran loading

To calculate the amount of TMR–dextran incorporated into the nanoparticles, 1 ml (20.1 mg/ml) dispersion was centrifuged at 20,000*g* and the sedimented particles were mixed with

1.0 ml of 0.2 M NaOH solution until a clear solution was observed (~48 h) at room temperature. After a second centrifugation at 20,000*g* for 28 min, the intensity of the fluorecence was measured at an emission wavelength of 577 nm (552 nm excitation) using a fluorescence spectrophotometer (Fluoro Max spectro-Fluorometer, Spex Industries Inc., New Jersey, USA). Additionally, a trypsin–EDTA solution (0.05%, Invitrogen Canada Inc., Burlington, ON, Canada) was used to release the TMR–dextran and to calculate the loading and the encapsulation efficiency. All fluorescent readings were analysed using a standard curve of TMR–dextran in PBS (pH 7.4).

2.3.2. In vitro release of TMR–dextran from nanoparticles

The 48 h release of TMR–dextran loaded nanoparticles was carried out in PBS, with and without enzyme (0.05% trypsin–EDTA), at 37 °C in a shaking water bath. 20.2 mg of sedimented TMR–dextran loaded gelatin nanoparticles were re-suspended in 1.0 ml of PBS or 1.0 ml of PBS containing enzyme. After different intervals of time, the particles were centrifuged and 500 μl of supernatant was removed. The PBS and trypsin containing PBS solutions were replaced each time in the respective vial containing nanoparticles to maintain the constant volume. The fluorescent intensity of the supernatant obtained at different time intervals was measured under the same conditions as described above in the loading study and the cumulative amount released was calculated from the appropriate calibration curves.

For all release studies, background fluorescent intensity reading was subtracted (i.e. fluorescent intensity readings for the unloaded nanoparticles treated in the same way as TMR–dextran loaded nanoparticles).

2.3.3. Isolation and culture of dendritic cells

DCs were generated from murine bone marrow cells by an established ex vivo culture method [21]. DCs were isolated from murine bone marrow cells by washing out the bone marrow 2–4 times and plating the cells in three Petri dishes (A, B and C), bacteriological grade 100 mm, each Petri dish at 2×10^6 cells in 10 ml RPMI-1640 media containing 200 ng of granulocyte macrophage colony stimulating factor (GM-CSF) (Peprotech, Rockville, MA, USA). The Petri dishes were then incubated at 37 °C and 5% CO_2 for 7 days. On days 3 and 6, culture media was replaced by fresh RPMI-1640 media containing 200 ng of GM-CSF and incubated the same way. It has been shown by previous studies in our lab with human DCs that day seven is the most efficient time for incubating DCs with particulate formulations [16]. Additionally, cellular uptake studies with PLGA nanoparticles by murine DCs have shown that the kinetics of the uptake is similar to that of human DCs (Elamanchili et al., personal communication, manuscript in preparation). Hence, on day 7, Petri dish 'A' was incubated with 200 μl of PBS, Petri dish 'B' with 200 μl of TMR–dextran (80 μg) in PBS, and Petri dish 'C' with 200 μl of nanoparticle dipersion (4.0 mg) in PBS that was loaded with 80 μg of TMR–dextran. All Petri dishes were then incubated for 24 h at 37 °C and 5% CO_2.

2.3.4. Flow cytometry (fluorescence activated cell sorting; FACS)

On day 8, after incubating with the formulations for 24 h, the cells from each Petri dish were harvested by gentle pipeting and aliquoted at 2×10^5 cells in microcentrifuge tubes containing cold staining buffer (PBS with 10% FBS and 0.05% sodium azide). For surface marker staining, titrated amounts of monoclonal antibodies specific for CD11c or MHC-II (Pharmingen, ON, Canada), or their respective isotype controls, were used. The cells were incubated at 4 °C for 30 min, washed three times and re-suspended in cold staining buffer. The cells were then incubated with fluorescein isothiocyanate (FITC) conjugated secondary antibodies (BD Pharmingen, ON, Canada) for 30 min at 4 °C. The cells were then washed with staining buffer, transferred to Falcon tubes and analyzed using a flow cytometer (Becton-Dickinson FACSort, Franklin Lakes, NJ, USA). A minimum of 10,000 events were collected. The data was analysed using Cell Quest analysis software (Becton-Dickinson) by gating on the live cell populations. In dual color flow cytometry studies, the compensation for fluorescence bleeding was routinely done using cells labelled with reagents having single fluorescence and by bringing the bleeding signals into their respective channels.

2.3.5. Confocal laser scanning microscopy

On day 7 in culture 2×10^5 dendritic cells in 300 μl media were transferred from Petri dish into each chamber of Lab-Tek II 8 slides (Nalgene Nunc Int., IL, USA). Control wells were pretreated with cytochalasin B (5 μg/ml) for 30 min. After the supernatant was removed from the cells they were incubated with 500 μl fresh media containing 20 μg of unlabeled gelatin nanoparticles, 20 μg of TMR–dextran loaded gelatin nanoparticles as well as soluble TMR–dextran. The control wells for the phagozytosis inhibition of these formulations contained cytochalasin B (5 μg/ml) during the complete study. After 24 h of incubation, the supernatants were removed and the cells were washed three times with 500 μl of PBS buffer and the membranes labeled by adding 100 μl of 0.0005% FITC-concanvalin A (Molecular Probes, OR, USA) solution in PBS buffer for 1–2 min. Before the fluorescent labeling of the cell membranes for the single cell images, the lysosomes were stained using 200 μl (50 nM) lysotracker blue DND-22 (Molecular Probes, OR, USA) for 30 min. Cell membranes were then labeled with a CD11c selective primary antibody and a secondary FITC labelled antibody. After three washings with PBS, the cells were fixed with 100 μl of 4% paraformaldehyde dissolved in PBS for 10 min. For nucleus labeling, the fixed cells were washed with PBS and further incubated for 15 min with 400 μl (2 μM) Hoechst 33342 dye (Molecular Probes, OR, USA). The cells were then finally washed with PBS, and the slides were prepared with a solution of 2.5% 1,4-Diazabicyclo [2.2.2.] octane (DABCO; Aldrich Chemical Company Ltd, WI, USA) and PBS/glycerol (1:1). The cells were examined using a confocal microscope Zeiss 510 LSMNLO (Carl Zeiss Microscope systems, Jena, Germany) with identical settings for each confocal study.

3. Results and discussion

Fluorescent macromolecular dye loaded gelatin nanoparticles were prepared for the following reasons. First, it is easy to analyze the drug loading and release with this fluorescent dye using fluorescence spectrophotometry. Secondly, it is easier to load the particles with fluorescent dyes as compared to other techniques including the use of radiolabeled proteins such as bovine serum albumin encapsulated in nanoparticles. Thirdly, the uptake of nanoparticles by DCs can be visualized using CLSM and, finally, the number of cells that have taken up nanoparticles can be analyzed by flow cytometry. The choice of the TMR–dextran was also based on its similarities in physicochemical characteristics with that of cancer antigens to be used in future studies. Several studies with various colloidal drug carrier formulations were already done in similar ways, but none with hydrophilic gelatin nanoparticles, which seems to have different intracellular distribution properties as compared to lipophilic polymer nanoparticles and liposomes.

3.1. Characterization of nanoparticles

3.1.1. Particle size analysis

The average particle size of unlabeled gelatin nanoparticles and TMR–dextran loaded gelatin nanoparticles was determined using photon correlation spectroscopy (PCS). The sizes found were 226 and 245 nm (mean of 10 subruns) with a narrow polydispersity index of 0.09 and 0.04, respectively (Table 1). The nanoparticles did not have any impurities with pyrogens (confirmed by endotoxin assay; data not shown).

3.1.2. Loading and in vitro release of TMR–dextran from nanoparticles

The loading efficiency of the fluorescent dye TMR–dextran was determined using fluorescence spectrophotometry. The loading efficiency was determined by two methods: (1) by alkaline hydrolysis of gelatin nanoparticles and (2) by enzymatic digestion of the nanoparticles using trypsin–EDTA as trypsin had shown earlier to be the most effective enzyme for the degradation of gelatin NP [22]. Both of the methods lead to the degradation of the gelatin nanoparticles. We assume that TMR–dextran was loaded to gelatin nanoparticles by forming strong interpenetrating networks between gelatin and dextran [23,24]. TMR–dextran would, therefore, be encapsulated during the co-acervation at a basic pH and during the last desolvation step. The TMR–dextran encapsulated in the gelatin nanoparticles, conducted by alkaline hydrolysis and by trypsin induced digestion, was calculated to be 18.7 and 13.4 μg per milligram gelatin, respectively, corresponding to 96.16 and 70.07%, respectively, of the TMR–dextran amount used for the encapsulation. Loading yield calculated by trypsin induced digestion of the nanoparticles was less as compared to the alkaline hydrolysis method. The higher values of the alkaline hydrolysis method, compared to the trypsin assisted digestion values, was probably caused by stronger background reading for the 'trypsin assisted method of degradation' than the 'alkaline hydrolysis method'. Additionally, there might be a linking of TMR–dextran molecules with degraded gelatin and non-degraded gelatin that prevented a complete release of the TMR–dextran by the enzyme assisted method.

Table 1
Particle size analysis and concentration of gelatin nanoparticles

Nanoparticle type	Size (nm)	PI[a]	Concentration (mg/ml)
Unloaded	226	0.09	20.5
TMR–dextran loaded	245	0.04	20.1

[a] PI, polydispersity index.

The release of TMR–dextran was performed in PBS alone, and in presence of trypsin–EDTA at 37 °C. Fig. 1, without enzymes, shows that there was just 0.6% release of the TMR–dextran after 12 h of shaking in a water bath; after 24 and 48 h there was a very low release of about 1.0% TMR–dextran. The results for diffusional release of TMR–dextran in our formulations were completely different as reported by Kaul et al., [25]. This difference can be due to a different preparation method of the TMR–dextran loaded gelatin nanoparticles. One example is that there was no addition of crosslinking agents such as glutaraldehyde in the method of preparing gelatin nanoparticles done by Kaul et al., [25]. If the gelatin nanoparticles prepared by our two-step desolvation technique are not crosslinked, when the media is changed into PBS buffer, they dissolve within several minutes and release the TMR–dextran. The addition of glutaraldehyde, which forms an inter- and intra-molecular crosslinking mostly on the surface of the gelatin nanoparticles leads to a hardening of the nanoparticles that causes a lower swelling and possibly the decrease of the TMR–dextran release by diffusion. In contrary, a release of 76.2% ($\pm$1.6%, $n=3$) after 24 h was achieved with the addition of trypsin–EDTA. Therewith we can predict that the later described release in tissue culture is probably not via passive diffusion; cellular enzymes must be responsible for the release. We did not see a complete release of TMR–dextran even after 72 h, as there might be some dextran that is still linked with parts of the gelatin/gelatin nanoparticles as already discussed above. The release characteristics observed was biphasic. This might be due to the surface crosslinking of the gelatin nanoparticles that can cause first an erosion of the

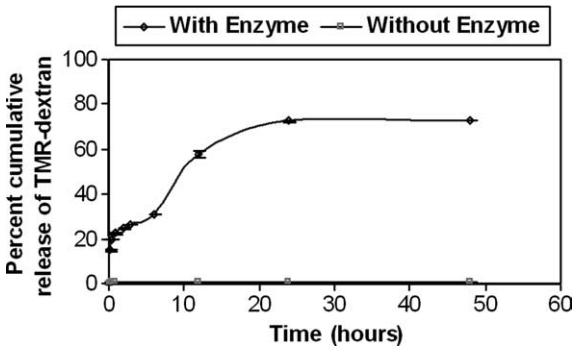

Fig. 1. In vitro release of TMR–dextran from gelatin nanoparticles in PBS with and without enzyme at 37 °C (mean $\pm$ SD; $n=3$).

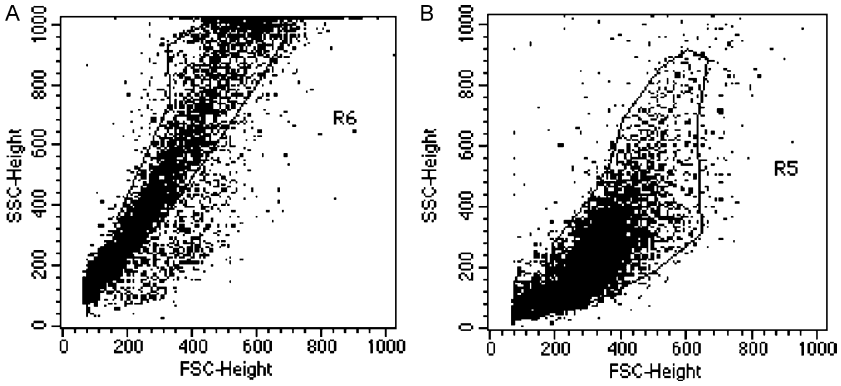

Fig. 2. Density plot for dendritic cells fed with (A) PBS and (B) TMR–dextran loaded gelatin nanoparticles. Side scatter indicates cell granularity or complexity. The forward scatter indicates the cell size.

nanoparticles in the core before a complete degradation of the nanoparticles started after about 6 h.

3.2. Uptake of gelatin nanoparticles by dendritic cells: Determination of the number of DCs taken up nanoparticles using flow cytometry

We quantitatively analyzed the phagocytosis using flow cytometry that provides information regarding the total number of DCs that have taken up gelatin nanoparticles. The nanoparticles used for the DC uptake studies were tested for their endotoxin levels using an endotoxin testing kit (QCL-1000, Bio-Whittaker, MD, USA) and were endotoxin free. After the incubation of TMR–dextran loaded gelatin nanoparticles to DCs, DCs ingested nanoparticles became granular. This can be seen by a shift of the cell population to high scatter, showing a changed granularity in the fluorescence activated cell sorting (FACS) density plot (Fig. 2). No change in the cellular granularity was seen when DCs were incubated with equivalent amounts of the soluble form of TMR–dextran. Only 4% of DCs were double positive for both CD11c and TMR–dextran. On the other hand 88% of DCs incubated with TMR–dextran loaded gelatin nanoparticles were double positive for both CD11c and TMR–dextran (Fig. 3); similar differences were seen for DCs with a MHC II specific labeling. 3% were double positive for MHC II and soluble TMR–dextran as compared to 87% in case of TMR–dextran loaded gelatin nanoparticles (Fig. 4). In Fig. 3, a FL-1 shift can also be seen after the incubation with TMR–dextran loaded nanoparticles. This new population is propably due to the change in the granularity as shown in Fig. 2 causing the increased FL-1 fluorescence intensity.

3.3. Uptake of gelatin nanoparticles by dendritic cells: Qualitative study using confocal laser scanning microscopy

Double and triple color confocal laser scanning microscopy (CLSM) was performed to determine the mechanism for the nanoparticles taken up by murine DCs and their intracellular location. Earlier studies with human DCs have shown that nanoparticles were taken up via phagocytosis [16]. Regarding murine DCs, we performed intensive CLSM-studies to confirm the uptake of different nanoparticulate formulations made of poly lactic-*co*-glycolic acid (PLGA), human serum albumin (HSA) and gelatin. For these studies, we concentrated on different layers in the *z*-axis. The results of these studies confirmed that PLGA and gelatin nanoparticles are taken up by murine DCs whereas nanoparticles made of HSA tended to adhere on the cell membranes [26]. Having these former studies in mind, we focused now on only one layer in the z-axis

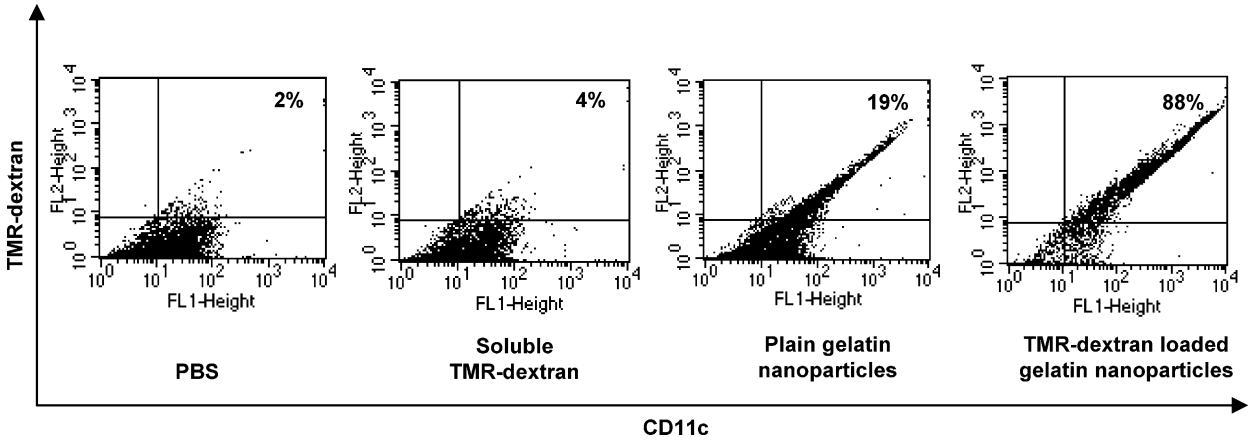

Fig. 3. Percentage of dendritic cells positive for CD11c (FL-1) and TMR–dextran (FL-2) following incubation with PBS, soluble TMR–dextran and TMR–dextran, plain gelatin nanoparticles and TMR–dextran loaded gelatin nanoparticles at 37 °C for 24 h.

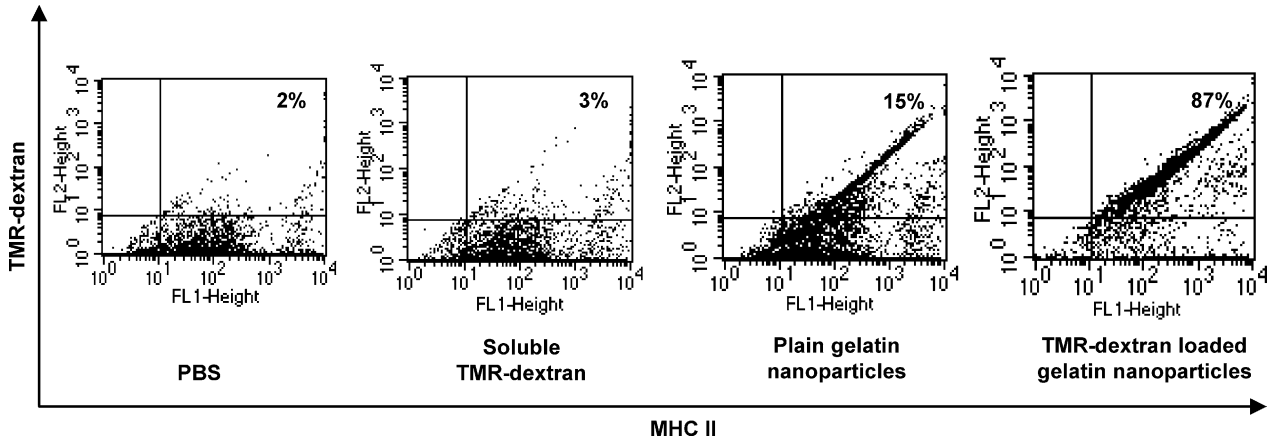

Fig. 4. Percentage of dendritic cells positive for MHC II (FL-1) and TMR–dextran (FL-2) following incubation with PBS, soluble TMR–dexran, plain gelatin nanoparticles and TMR–dextran loaded gelatin nanoparticles at 37 °C for 24 h.

that was more or less in the middle of the imaged cells depending on the cells size (Figs. 5–7). Our first aim was to confirm the former results on human DCs [16] for murine DCs. In Fig. 5(A), the murine DCs were only stained with Alexa 488 Concanavalin A. Fig. 5(B) shows DCs incubated with TMR–dextran loaded gelatin NP where DCs were treated with the pagocytosis inhibitor cytochalasin B where no cellular uptake could be observed. Incubating the DCs with soluble TMR–dextran shows just a minor uptake that correlates with our FACS data (Fig. 5(C)). Finally in Fig. 5(D), DCs were incubated with TMR–dextran loaded gelatin nanoparticles which results in a cellular uptake correlating also with the

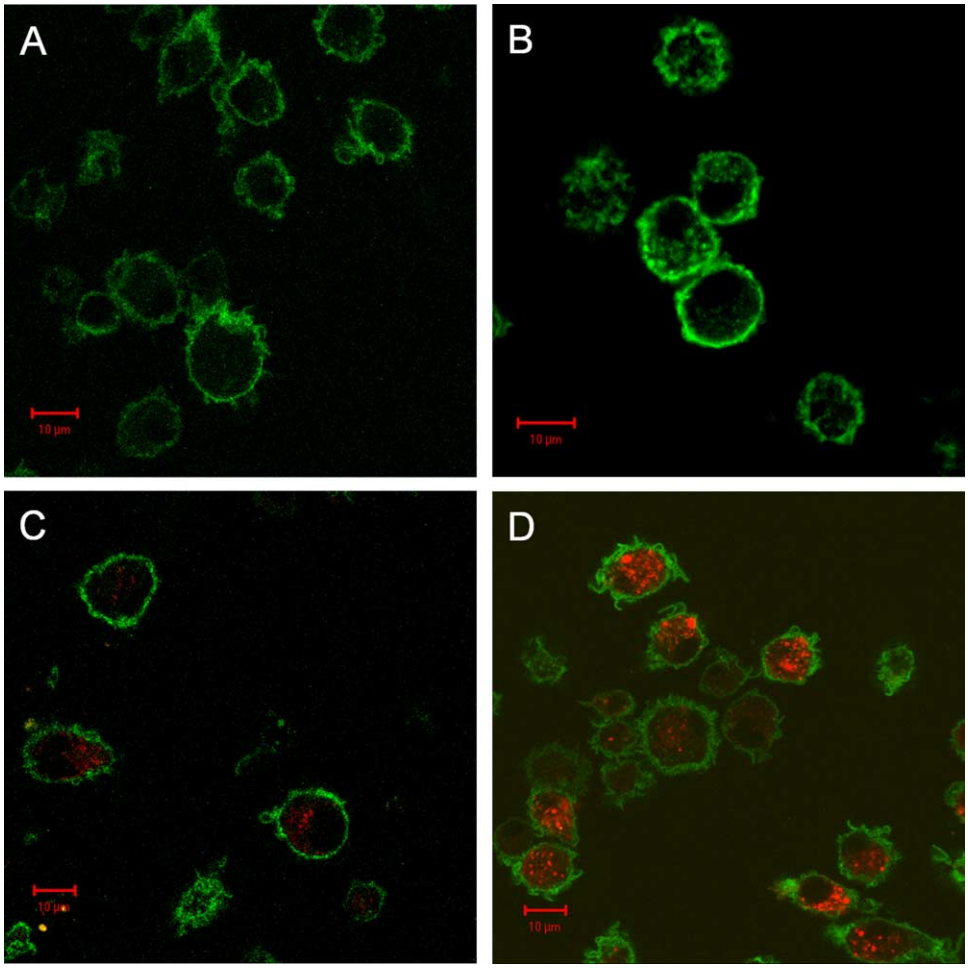

Fig. 5. Cellular uptake of TMR–dextran loaded gelatin nanoparticles (red label) in dendritic cells. (A) Dendritic cells incubated with PBS, (B) Cytochalasin B pretreated dendritic cells incubated with TMR–dextran loaded nanoparticles, (C) Dendritic cells incubated with soluble TMR–dextran, (D) Dendritic cells incubated with TMR–dextran loaded nanoparticles; DC membranes (A, B, C, D) were stained with Alexa 488 Concanavalin A (green).

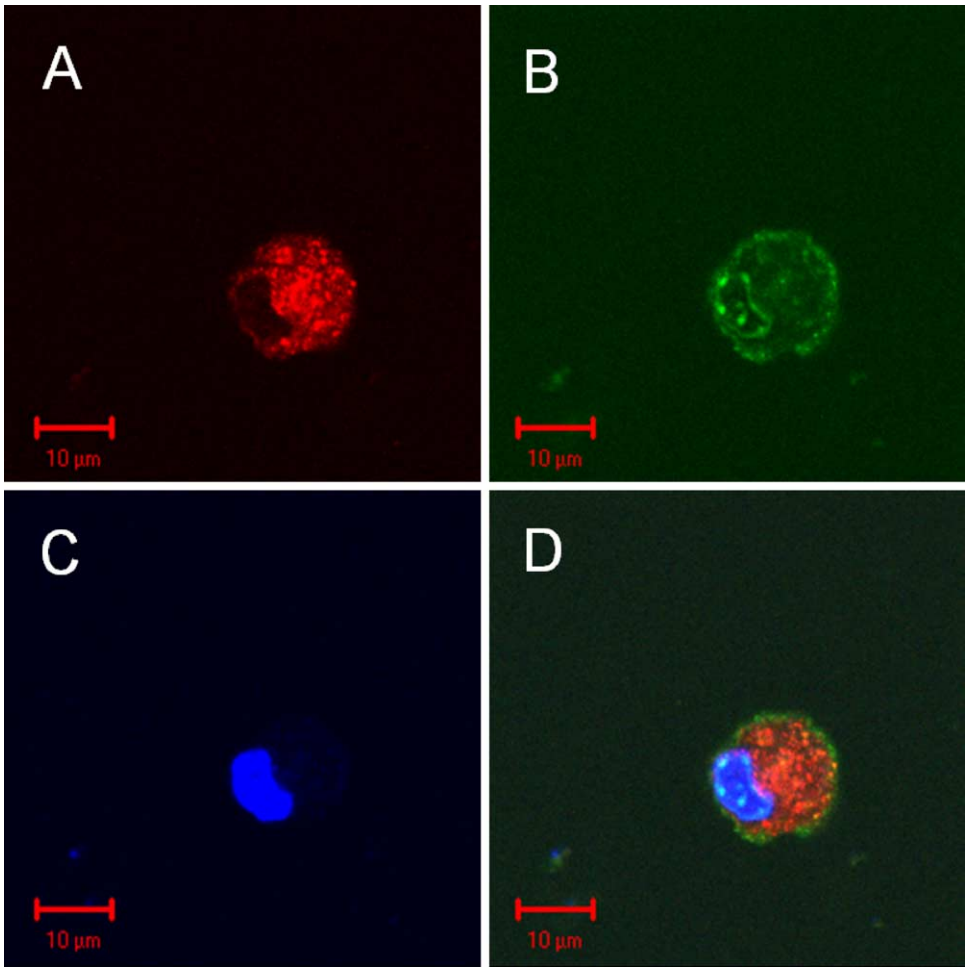

Fig. 6. Single cell image of a dendritic cell incubated with TMR–dextran loaded nanoparticles. (A) TMR–dextran labelled gelatin nanoparticles (red label), (B) cell membrane stained with FITC primary/secondary antibody to CD11c (green label), (C) nucleus staining (blue label), (D) overlay of A, B and C.

FACS analysis. Until here, the study showed the expected results from our earlier studies [16,26]. The challenging part of this study was to perform a single cell imaging to achieve more details on the intracellular distribution of the TMR–dextran loaded gelatin nanoparticles. For this study, we used a triple color staining. We stained two cellular compartments, the nucleus (Fig. 6(C)) and the lysosomes (Fig. 7(C)), in addition to the labeled nanoparticles and the cell membranes. The population of murine DCs using the method of Lutz et al. [21] leads mostly to approximately 90% DCs as also shown in our CD11c positive gated population in the FACS analysis. Hence, for the CLSM imaging of populations between 5 and 12 cells as shown in Fig. 5, a non-specific membrane staining is possible when the cell population was previously analyzed with a specific murine DC marker. For single cell imaging this method is impossible because there remains a small chance that not a DC is imaged. For this reason we have chosen the primary/secondary antibody CD11c staining, along with the isotype controls, to confirm that the imaged cell is a murine DC. Therefore, the membrane staining in Figs. 6(B) and 7(B) is not as clear as in Fig. 5. We chose to present the single cell imaging by showing each fluorescent channel separately (Figs. 6(A), (B) and (C) and 7(A), (B) and (C)) and then the overlay of all three (Figs. 6(D) and 7(D)) to demonstrate a good channel separation with minor interferences. Fig. 6, clearly shows that after an incubation of 24 h TMR–dextran labeled gelatin nanoparticles cannot be found in the nucleus. Based on the overlay (Fig. 6(D)), it can be assumed that some of the nanoparticles are in endo-lysosomes close to the nucleus. Although the results of Fig. 6 seem to be predictable for a hydrophilic colloidal drug carrier system, like gelatin nanoparticles, it has never been conclusively demonstrated previously. Based on the general understanding that colloidal drug carrier systems taken up by phagocytosis remain in the endo-lysosomes, we would expect that the finding in Fig. 7 is most likely a complete co-localization of the TMR–dextran loaded gelatin nanoparticles with the lysotracker stained lysosomes. It is obvious that Fig. 7(A) and (C) show a co-localization of the blue stained lysosomes and the red labeled gelatin nanoparticles. But a closer look at the overlay (Fig. 7(D)) also shows a clear blue fluorescence that is not co-localized with the red stained nanoparticles. This information confirms that not all lysosomes are involved in the uptake process. The most interesting finding is that there is still red fluorescence that is not co-localized with the blue stained lysosomes. Although the red fluorescence in the upper part of

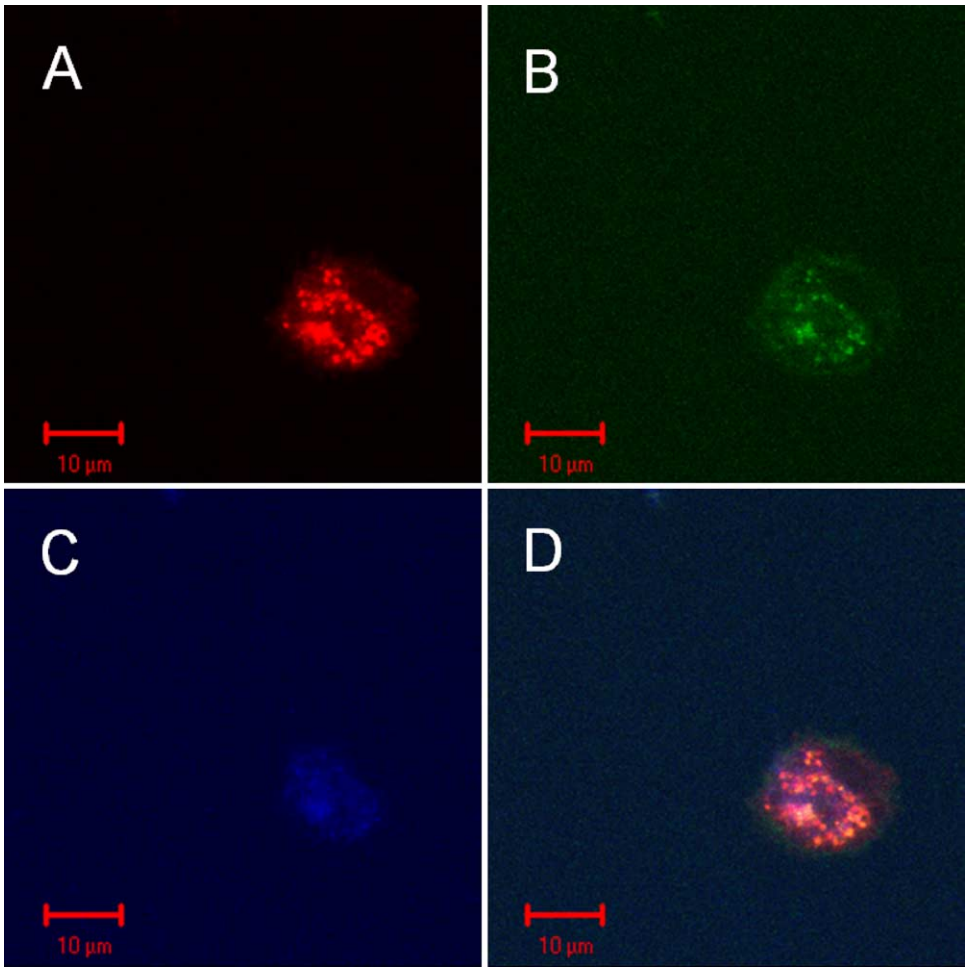

Fig. 7. Single cell image of a dendritic cell incubated with TMR–dextran loaded nanoparticles. (A) TMR–dextran labelled gelatin nanoparticles (red label), (B) cell membrane stained with FITC primary/secondary antibody to CD11c (green label), (C) lysosomal staining (blue label), (D) overlay of A, B and C.

the cell interferes with the green membrane staining and therewith is more orange than red in the overlay, from the several single cell images obtained, we can assume that gelatin nanoparticles are not completely stuck in lysosomes after 24 h of incubation. The red fluorescence outside the endolysosomes may represent TMR–dextran released as result of the enzymatic degradation of the nanoparticles and then escaped into the cytoplasm. This possibility is supported by the results of the trypsin assisted degradation of the nanoparticles in vitro, showing the release of approximately 80% TMR–dextran within 24 h. Alternatively, some intact nanoparticles might have escaped into the cytoplasm as a result of disruption of endolysosomal membrane. Preliminary results of our recent collaborative study with Prof. Vollmar (Department for Pharmaceutical Biology in Munich, Germany), on the subcellular trafficking of gelatin nanoparticles support this view. A successful inhibition of NF-κB in the cytoplasm with decoy oligonucleotide loaded gelatin nanoparticles, observed in that study (unpublished results), is also consistent with either of the above possibilities. At present, we are unable to conclusively answer the question whether the red fluorescence in the cytoplasm was due to the intact TMR–dextran loaded gelatin nanoparticles or the released fluorescent probe. However, the granular appearance of the fluorescence suggests the former. Nevertheless, both possibilities raise new questions on the escape mechanisms of the drugs encapsulated in hydrophilic colloidal drug carrier systems based on gelatin from the lysosomes, and 'non-classical' alternate pathways of uptake of gelatin nanoparticles by DCs. More detailed imaging and kinetic studies are required to further confirm our results and provide mechanistic insights on the cellular uptake and intracellular trafficking of gelatin nanoparticles. Several such studies, especially the mechanisms of intracellular trafficking of colloidal drug carrier systems, are currently in progress.

4. Conclusions

This study, for the first time, conclusively demonstrated the uptake of gelatin nanoparticles by murine bone marrow DCs. The internalization of the fluorescent probe (TMR–dextran) in gelatin nanoparticles was higher than that of the soluble form. The internalized nanoparticles were mostly localized in the lysosomes, with some escape into the cytoplasm, but no localization in the nucleus. Overall, these results suggest that gelatin nanoparticles are suitable for targeting antigens to DCs

and deserve further evaluation in vivo as a safe and effective vaccine delivery system.

Acknowledgements

We thank Praveen Elamanchili for performing the endotoxin tests and his support in the ex vivo isolation and preparation of the murine DCs. This project was funded by grants from the Natural Sciences and Engineering Research Council of Canada (STPGP 258032) and Canadian Institute of Health Research (MOP 42407).

References

[1] G. Marland, A.B. Bakker, G.J. Adema, C.G. Figdor, Dendritic cells in immune response induction, Stem Cells 14 (1996) 501–507.
[2] C.V. Harding, R. Song, Phagocytic processing of exogenous particulate antigens by macrophages for presentation by class I MHC molecules, J. Immunol. 153 (1994) 4925–4933.
[3] C. Reis e Sousa, J.M. Austyn, Phagocytosis of antigens by Langerhans cells, Adv. Exp. Med. Biol. 329 (1993) 199–204.
[4] M. Diwan, M. Tafaghodi, J. Samuel, Enhancement of immune responses by co-delivery of a CpG oligodeoxynucleotide and tetanus toxoid in biodegradable nanospheres, J. Control. Release 85 (2002) 247–262.
[5] P. Elamanchili, M. Diwan, M. Cao, J. Samuel, Characterization of poly(D, L-lactic-*co*-glycolic acid) based nanoparticulate system for enhanced delivery of antigens to dendritic cells, Vaccine 22 (2004) 2406–2412.
[6] C. Scheicher, M. Mehlig, H.P. Dienes, K. Reske, Uptake of microparticle-adsorbed protein antigen by bone marrow-derived dendritic cells results in up-regulation of interleukin-1 alpha and interleukin-12 p40/p35 and triggers prolonged, efficient antigen presentation, J. Immunol. 25 (1995) 1566–1572.
[7] I.M. Svane, M.L. Soot, S. Buus, H.E. Johnsen, Clinical application of dendritic cells in cancer vaccination therapy, Apmis 111 (2003) 818–834.
[8] M. Gregoire, C. Ligeza-Poisson, N. Juge-Morineau, R. Spisek, Anticancer therapy using dendritic cells and apoptotic tumour cells: preclinical data in human mesothelioma and acute myeloid leukaemia, Vaccine 21 (2003) 79179–79184.
[9] M. Jefford, E. Maraskovsky, J. Cebon, I.D. Davis, The use of dendritic cells in cancer therapy, Lancet Oncol. 2 (2001) 343–353.
[10] J.M. Timmerman, R. Levy, Dendritic cell vaccines for cancer immunotherapy, Annu. Rev. Med. 50 (1999) 507–529.
[11] J. Banchereau, F. Briere, C. Caux, J. Davoust, S. Lebecque, Y.J. Liu, B. Pulendran, K. Palucka, Immunobiology of dendritic cells, Annu. Rev. Immunol. 18 (2000) 767–811.
[12] C.A. Janeway, P. Travers, M. Walport, M.J. Shlomchik, The Immune System in Health and Disease, Garland Publishing, New York, 2001.
[13] E.G. Engleman, Dendritic cells: potential role in cancer therapy, Cytotechnology 25 (1997) 1–8.
[14] G. Murphy, B. Tjoa, H. Ragde, G. Kenny, A. Boynton, Phase I clinical trial: T-cell therapy for prostate cancer using autologous dendritic cells pulsed with HLA-A0201-specific peptides from prostate-specific membrane antigen, Prostate 29 (1996) 371–380.
[15] J. Kreuter, Nanoparticulate systems in drug delivery and targeting, J. Drug Target. 3 (1995) 171–173.
[16] M.E. Lutsiak, D.R. Robinson, C. Coester, G.S. Kwon, J. Samuel, Analysis of poly(D,L-lactic-*co*-glycolic acid) nanosphere uptake by human dendritic cells and macrophages in vitro, Pharm. Res. 19 (2002) 1480–1487.
[17] H.G. Schwick, K. Heide, Immunochemistry and immunology of collagen and gelatin, Bibl. Haematol. 33 (1969) 111–125.
[18] M. Fujii, Angioarchitectural studies of canine optic nerve. Report 1: gelatin injection technique, Nippon Ganka Gakkai Zasshi. 87 (1983) 65–69.
[19] N. Tanigawa, T. Shimomatsuya, K. Takahashi, Y. Inomata, K. Tanaka, K. Satomura, Y. Hikasa, M. Hashida, S. Muranishi, H. Sezaki, Treatment of cystic hygroma and lymphangioma with the use of bleomycin fat emulsion, Cancer 60 (1987) 741–749.
[20] C.J. Coester, K. Langer, H. van Briesen, J. Kreuter, Gelatin nanoparticles by two step desolvation–a new preparation method, surface modifications and cell uptake, J. Microencapsul. 17 (2000) 187–193.
[21] M.B. Lutz, N. Kukutsch, A.L. Ogilvie, S. Rossner, F. Koch, N. Romani, G. Schuler, An advanced culture method for generating large quantities of highly pure dendritic cells from mouse bone marrow, J. Immunol. Methods 223 (1999) 77–92.
[22] E. Leo, M.A. Vandelli, R. Cameroni, F. Forni, Doxorubicin-loaded gelatin nanoparticles stabilized by glutaraldehyde: involvement of the drug in the cross-linking process, Int. J. Pharm. 155 (1997) 75–82.
[23] R. Cortesi, E. Esposito, M. Osti, G. Squarzoni, E. Menegatti, S.S. Davis, C. Nastruzzi, Dextran cross-linked gelatin microspheres as a drug delivery system, Eur. J. Pharm. Biopharm. 47 (1999) 153–160.
[24] J.D. Kosmala, D.B. Henthorn, L. Brannon-Peppas, Preparation of interpenetrating networks of gelatin and dextran as degradable biomaterials, Biomaterials 21 (2000) 2019–2023.
[25] G. Kaul, M. Amiji, Long-circulating poly(ethylene glycol)-modified gelatin nanoparticles for intracellular delivery, Pharm. Res. 19 (2002) 1061–1067.
[26] P. Elamanchili, J. Samuel, C. Coester, Cellular uptake of three different biodegradable nanoparticles by murine bone marrow-dendritic cells: an *in vitro* study, Proceedings of the 4rd World meeting on Pharmaceutics, Biopharmaceutics and Pharmaceutical Technology, 8–11 April 2002, Florence, Italy.